

# Anatomical traits of *Cryptomeria japonica* tree rings studied by wavelet convolutional neural network

T Nakajima<sup>1\*</sup>, K Kobayashi<sup>2</sup> and J Sugiyama<sup>1\*,3</sup>

<sup>1</sup> Research Institute for Sustainable Humanosphere, Kyoto University, Uji Kyoto 611-0011, Japan

<sup>2</sup> Graduate School of Agricultural and Life Sciences, The University of Tokyo, Tokyo 113-8657, Japan

<sup>3</sup> College of Materials Science and Engineering, Nanjing Forestry University, Nanjing 210037, China

E-mail: nakajima.takeshi.66z@st.kyoto-u.ac.jp, sugiyama.junji.6m@kyoto-u.ac.jp

**Abstract.** Tree ring analysis is an important field of science, and is vital in modeling the environmental response system of tree growth. In most cases, analyses have been conducted using one parameter from one tree ring, e.g., ring-width, density, or ratio of stable isotopes. The information within a ring, however, has been less studied, although it offers many more possibilities for investigation, such as seasonal responses over shorter time scales. Therefore, to elucidate the sub-seasonal climatic response of softwood (*Cryptomeria japonica*), we investigate the use of a wavelet-convolutional neural network (CNN) model, which incorporates spectral information that is normally lost in conventional CNN models. This paper highlights the usefulness of the wavelet-CNN for classifying cross-sectional optical micrographs and extracting structural information specific to a calendar year. Class activation maps indicate that the dimension and position of cells in a radial file are likely to be discriminative features for the wavelet-CNN. This study shows that wavelet-CNNs have the potential to be highly effective methods for dendrochronology.

## 1. Introduction

Tree ring analysis is an important task in many fields, including dendrochronology, dendroclimatology, and modeling the tree growth environmental response systems [1]. In these studies, tree ring widths have been used as the main feature for analyzing the relationships between tree growth and climate and for reconstructing past long-term climatic change. At the same time, there have been several attempts to extract much finer seasonal responses within an annual ring [2] [3]. For example, the structure of hardwood, which is more differentiated anatomically than that of softwood. Among the many anatomical features in this structure, vessel parameters are considered to be the best promising proxies for seasonal dendroclimatic analysis [4] [5].

In contrast, the structure of softwood, which is simpler, more regular and periodic, the structural signature is not obvious. However, recent analysis has suggested that the changes of wood density from earlywood to latewood [6] or radial diameters and cell wall thickness in a radial file could reflect well the intra-annual seasonal responses [7]. The information within a ring, however, is expected to be much more complex, and it seems difficult to reach a general conclusion from visual inspection or a



limited number of measurements. Given this situation, we have employed deep-learning in the field of tree ring analysis.

In recent years image recognition technology has improved and has been applied in various fields. It is also applied to the field of wood science especially in species (wood) identification. Several methods such as the gray level co-occurrence matrix [8, 9], local binary patterns [10, 11], and higher order local autocorrelation [12] have been employed to extract features from wood images. Identification with high accuracy was achieved using these features extracted from various types of images such as stereomicrographs, optical micrographs, or images from 3D computed X-ray tomography. More recently, Scale-Invariant Feature Transform (SIFT) [13], which are robust features based on the local density gradient, were used to analyze optical micrographs of family Lauraceae [14]. The result indicates that the classification can be performed with precision, and features specific to the species provide anatomical implications so far unreported as a result of visual inspection. This conclusion was further confirmed by employing bag-of-feature models of SIFT descriptors [15]. These studies strongly suggest the applicability of computer vision as a new tool for wood anatomy.

In addition to the above conventional machine learning approaches using manually designed feature extractors and classifiers, CNNs have also been tested. In addition to Lauraceae, about 8,000 images from six classes and 51 genera were used to form a hardwood image database that was tested by VGG16 model and its modified form. The resulting accuracy was excellent; however, when the same model was applied to the softwood database (e.g., pine and cypress) it was no better than visual inspection [16].

As already mentioned, softwood appearance is simpler and more regular than that of the hardwood. Similar to many algorithms, CNNs process images directly in the spatial domain; thus, a CNN is considered to be an essentially spatial approach [17]. In contrast, spectral information such as repetition and periodicity is another important type of image information, particularly in the case of softwood images. Therefore, to include both spatial and spectral information, a combined model consisting of the wavelet transform and a CNN (wavelet-CNN) [17] was examined in this study.

In this paper, we report the results of calendar year predictions using two strategies, namely wavelet-CNN analysis using optical microscopic images and a random forest classifier with 21 anatomical features estimated from each ring. The performance of wavelet-CNN is evaluated against the results obtained by random forest analysis.

## 2. Material and methods

### 2.1 Wood material

Three wood disks from Japanese cedar (*Cryptomeria japonica*, D. Don) planted in the Ashiu Experimental Forest, Field Research Center, Kyoto University, were investigated. The trees fell during the typhoon in 2017 and consists of the around 70 years annual rings up to 2017. In addition, a precise meteorological data of the site is available for the future ring-climate correlation analysis. For each wood disk, wood blocks from four different radial directions were collected, and assigned labels A to D.

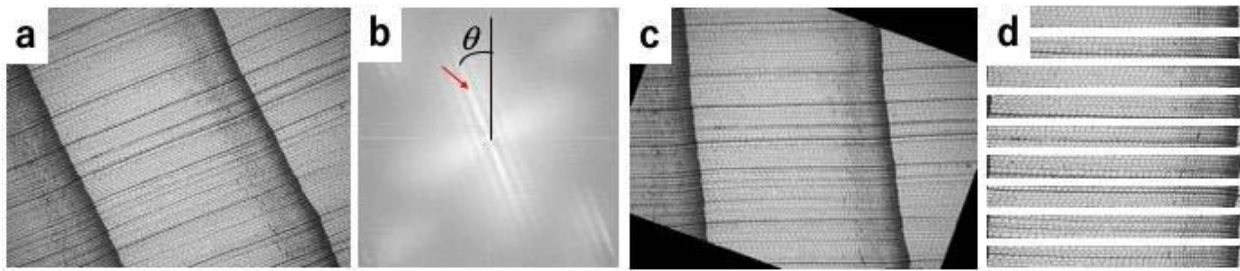


Figure 1. Series of image preprocessing steps. a) Original image, b) power spectrum of (a), c) image after rotation, and d) images after cropping and resizing.

From each wood block, transverse sections (20  $\mu\text{m}$  thick) were prepared using a sliding microtome (Yamato, Japan) and the wood surface was covered with a corn starch solution. The quality of the transverse sections was greatly improved using this method, because it significantly decreases the incidence of secondary cell walls splitting off the primary wall while making transverse sections [18]. After preparing the transverse sections, they were stained with 0.5% safranin solution. These sections covered 18 annual rings (2000–2017) in all directions from each wood disk.

Then, the cross-sectional images were acquired with an Olympus™ 2 $\times$  (0.08 NA) PlanApo objective lens using a BX51 optical microscope equipped with a DP73 charge-coupled device camera. The original image was RGB color and had a size of 1600  $\times$  1200 pixels with a pixel resolution of 2.2  $\mu\text{m}$ .

## 2.2 Image preprocessing

One of the most striking differences between hardwood and softwood is that the softwood cells (tracheids) are perfectly aligned along the radial directions. These series of cells are generated by the cell division of the same cambial initials and called radial files. Assuming that each radial file must contain seasonal memory of the climate, the radial files are aligned horizontally as precisely as possible. For this purpose, the Fourier transform is used, as shown in Figure 3b, to find the angle between the vertical axis of the image and the maximum intensity of the streak that appears perpendicular to the radial files in the power spectrum (indicated by the arrow). After rotating an image by, as shown in Figure 3c, density profiles along the horizontal directions were measured and the annual ring borders were located. Then, smaller images covering one annual ring were cropped and reshaped into 80  $\times$  800 (height  $\times$  width) pixel images. The resulting images form the final image database, which is summarized in Table 1.

Table 1. Summary of the image database

Sample	AS_1				AS_2				AS_3			
	A	B	C	D	A	B	C	D	A	B	C	D
Direction	A	B	C	D	A	B	C	D	A	B	C	D
Years included	18	18	17	17	18	18	18	18	17	17	18	17
Total image number	919	921	942	944	1585	913	1147	1235	1251	1395	1359	1384
Average image number / year	51.1	51.2	55.4	55.5	88.1	50.7	63.7	68.6	73.6	82.1	75.5	81.4

## 2.3 Wavelet-CNN model

Of the several existing networks, the wavelet-CNN recently proposed by Fujieda et al. [9] is investigated in the present analysis. In this study, Haar wavelets are used as the mother wavelet. Because Haar wavelets are orthogonal functions, they are suitable for representing radial and tangential

properties; tangential and radial cell walls appear as discrete signals and are almost aligned in either the vertical or horizontal direction. Based on the above points, each image was divided into four different frequency blocks after wavelet transformation. These LL, HL, LH, and HH blocks are shown in Figure 2. In this research, the LL and HL blocks were included in the wavelet-CNN to obtain information about the transition of radial cell walls, which reflects the annual growth pattern in the target calendar year. Up to five levels of image wavelet decompositions were extracted, as shown in Figure 2. Clearly, images of levels 1–3 appear to contain information about the specific patterns in radial files; the average resolution of one pixel is estimated to be 4.4  $\mu\text{m}$  (level 1), 9  $\mu\text{m}$  (level 2), 18  $\mu\text{m}$  (level 3), 36  $\mu\text{m}$  (level 4), and 72  $\mu\text{m}$  (level 5). This also means that three levels were the upper limit for detecting cells in a radial file. Thus, in this research, the original tree ring images and those after 1–3 levels of wavelet decomposition were trained using the wavelet-CNN.

For the first training–testing division, 17% of the dataset were used as test data, maintaining equal proportions of each directional dataset, and the rest formed the training dataset. Three evaluation methods were prepared. First, the test set included only one directional data image and we examined how the wavelet-CNN extracted year-specific features from each directional dataset. Secondly, the test set included data from one individual and we tested whether the wavelet-CNN could extract year-specific features from each individual wood disk, beyond directional anisotropy. Finally, the test set included all original test data and we tested whether the wavelet-CNN could extract year-specific features beyond individual differences. Validation was performed using the 17% of data in the training set, and the models constructed after 100 epochs (repetition of training) were evaluated using the test set. The whole process was repeated three times. All programs were written in Python 3.6 using the Keras and TensorFlow libraries.

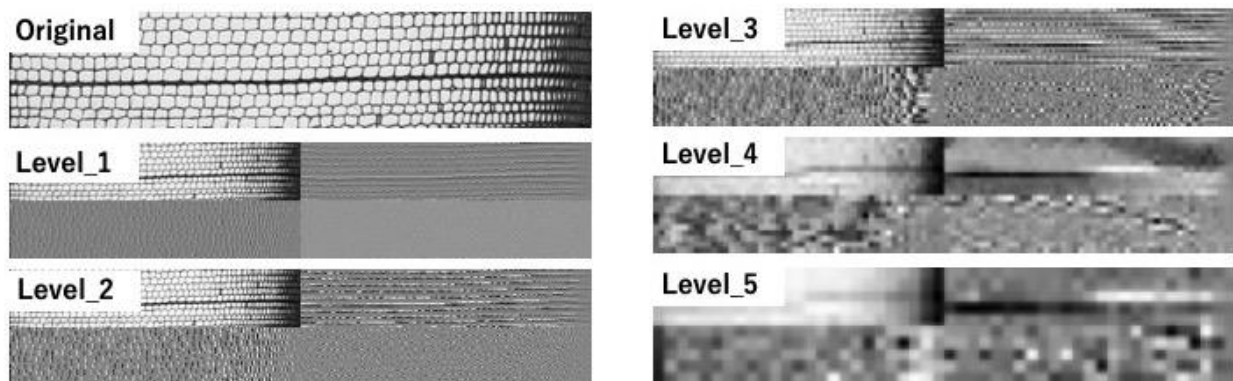


Figure 2. Example of a discrete wavelet transform decomposition. At each level, four different frequency blocks, LL, HL, LH, and HH, are shown at the top-left, bottom-left, top-right, bottom-right, respectively. L: low frequency, H: high frequency. The average resolution of one pixel is estimated to be 4.4  $\mu\text{m}$  (level 1), 9  $\mu\text{m}$  (level 2), 18  $\mu\text{m}$  (level 3), 36  $\mu\text{m}$  (level 4), and 72  $\mu\text{m}$  (level 5). In the wavelet-CNN used in this research, only LL and HL are included.

#### 2.4 Anatomical feature and random forest

We calculated anatomical feature parameters from each tree ring micrographs with the original ring widths. Tree ring images were binarized using Otsu's criteria [19]. Anatomical features such as lumen area, lumen radial diameter (LRD), and the centroid coordinates of cell lumen were then calculated using the Connected Component routine from the Python library. The wall radial thickness (WRT) of the cells was calculated using the LRD and the centroid coordinates of cell lumen. We present an example of calculating the WRT of Cell\_1 in Fig. 3(d) from the anatomical features of two adjacent cells, Cell\_1 and Cell\_2. WRT is the average value (half) of the difference between the centroid

distance  $d(C_1C_2)$  and the corresponding lumen length ( $\frac{LRD_1+LRD_2}{2}$ ). In this calculation, we assume that adjacent WRTs have the same value and that the WRT of the target cell (Cell\_1) is equal to the right-hand WRT next to the target cell lumen. The above description can be expressed by the following equation:  $WRT = \left[ d(C_1C_2) - \frac{LRD_1+LRD_2}{2} \right] / 2$ . At this point, accidentally connected regions were excluded as outliers. Such regions include those where the lumen size is greater than  $50 \mu\text{m}$  in height or  $60 \mu\text{m}$  in width, and areas with a lumen size of less than  $10 \mu\text{m}$  width that are positioned  $4/5$  of the tree ring width from the earlywood boundary, or have an aspect ratio of less than 0.5 (height/width) or greater than 3, which are considered to be noise. These threshold data on *Cryptomeria japonica* are taken from [20]. The annual ring images were then divided into ten equal portions. From each portion, we calculated the average LRD and cell WRT (20 parameters) and the tree ring width. Thus, a total of 21 parameters were taken from each tree ring image. The LRD, WRT, and ring width values were then standardized. In this research, several methods used in general tree ring analysis, such as constructing the chronology or detecting the growth trend, were not used.

Calendar year prediction was conducted using a random forest approach. In recent years, research using machine learning instead of traditional linear models has increased, with several machine learning techniques outperforming linear models [21]. Thus, we decided to use the random forest classifier, which is a machine learning method, to evaluate the contribution of each important feature to the result. The training and test data were divided in the same way as described in section 2.3.

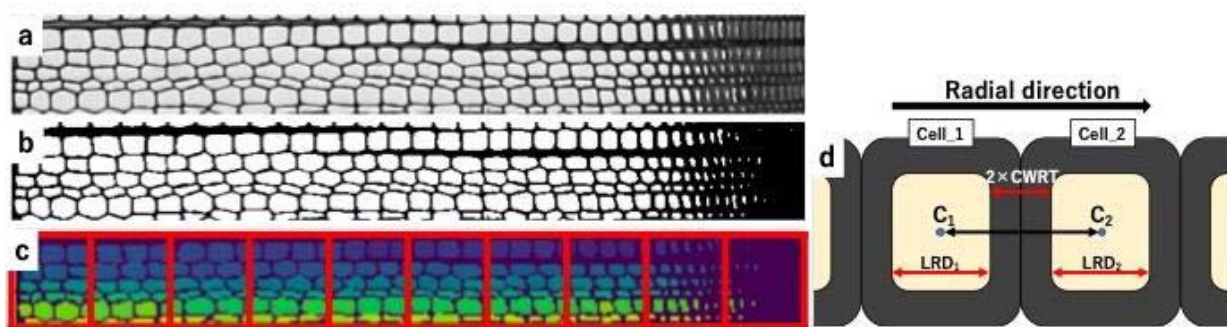


Figure 3. Series of image processing steps for calculating anatomical features. a) Original image, b) image binarized using Otsu's method, c) calculating lumen radial diameter (LRD) and centroid coordinates of cell lumen by Connected Component method, and d) representation of a schematic radial file of two adjacent cells and calculating cell wall radial thickness (WRT) using LRD and centroid coordinates of cell lumen.

### 3. Result and discussion

#### 3.1 Effect of radial position on prediction accuracy

The results of calendar year prediction using the wavelet-CNN and random forest approaches are presented in Table 2. First, the wavelet-CNN accuracy averages more than 70%. This is an amazing result because comparative classifiers using VGG-like models, which have not been described in detail in this paper, cannot achieve accuracy levels above 15%. VGG-like models only conduct species identification of hardwood, but wavelet-CNN can predict the calendar year from tree ring images taken from one species, *Cryptomeria japonica*, that are slightly different but very similar to each other. There were some differences in accuracy for each direction, especially in AS\_1.

We mixed all the image data taken from different radial directions of the three wood disks and repeated the tests. Because of the directional anisotropy of wood, even in an image set from the same

year, the rings vary in width, i.e., there are different numbers of cells in the radial files. This is because the annual rings are not exactly concentric and the growth is directionally different. However, to our surprise, the wavelet-CNN provided an accuracy of around 75%. This indicates that the computer vision approach can successfully detect so-far unknown sub-seasonal rhythms in radial files that are sufficiently discriminative to mitigate the directional fluctuation of radial growth and individual differences.

Secondly, the accuracy of the random forest classifier and anatomical features was examined. The calendar year prediction using the random forest achieves an accuracy of around 50–60% when testing each individual and 46% when testing all of the mixed test data. It is remarkable that only 21 measured values can achieve over 50% accuracy in calendar year prediction, and several tree ring studies using such tree growth parameters have reported interesting correlations between annual growth patterns and climate information [7]. Based on this fact, there is a strong chance that wavelet-CNNs could be used to provide deeper insights in the field of tree ring research.

Table 2. Accuracy of calendar year prediction using wavelet-CNN and random forest classifier

Direction for test data	A	B	C	D	Wavelet-CNN Average	Random Forest
AS_1	67.5	76.0	62.0	81.5	73.4	53.7
AS_2	77.2	75.0	75.5	75.7	77.7	62.0
AS_3	82.0	87.7	84.3	84.7	80.3	56.9
ALL data mixed					75.1	46.0

### 3.2 Attentional area for the prediction

Using the final convolutional layer of the wavelet-CNN model, gradient–class activation map (Grad-CAM) images were obtained following the method proposed by Selvaraju et al. [22] in order to see the place where network was excited. Typical images, together with the corresponding CAMs from all directions of AS\_1 in 2004, are presented in Figure 4. The upper images for each direction represent the original tree ring image and the lower images represent the rational judgements of the upper images made by Grad-CAM. Red parts are those that are important in determining the correct year. The reason why these upper and lower images represent the same tree ring image but the ring widths are different is that the lower images have been reshaped to have a width of 800 pixels so that all tree ring images are the same size. Intriguingly, the regions of attention are found in very similar radial positions in the annual rings, and the area where the cell wall is thicker than the surrounding area in the transition zone from earlywood to latewood receives significant attention in all images.

The phenomenon whereby cell walls in particular areas are thicker than those in surrounding areas can be considered as the tree growth activity being occasionally weakened by harsh drying during midsummer, then refreshed by off-seasonal late summer precipitation. In this case, the normal transition from earlywood to latewood can be modulated in such a way that a partial recovery from latewood to earlywood occurs. Usually, such a minor modulation is not noticeable by visual inspection. This study has, however, elegantly demonstrated for the first time that the modulation and its position can be a discriminative feature of the calendar year.

Variation within a ring is sufficiently large to be greater than the variation among different rings. As a potential method of normalizing this difference to allow for comparison, we resized all the images to  $80 \times 800$  pixels. However, more work is needed on the data normalization along the radial direction to preserve the time scale as precisely as possible.

Although there are still several important issues to overcome, the applicability of wavelet-CNNs is promising. In particular, such models will shed light on softwood identification, which has so far been difficult using conventional CNNs such as VGG-like models. Work along these lines is also in progress.



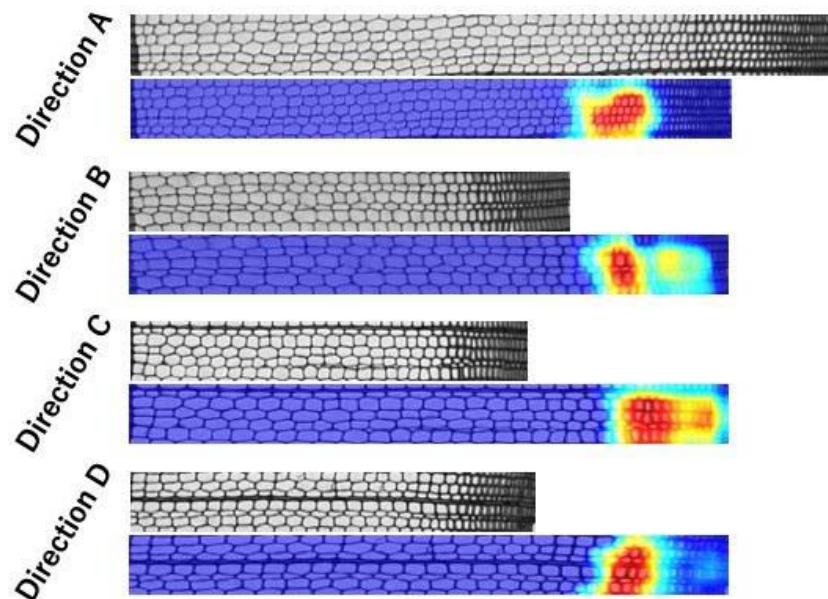


Figure 4. CAMs using the final convolutional layer [18] in our wavelet-CNN. The highlighted area indicates the discriminative image regions used by the network to identify the corresponding calendar year. In the case of AS\_1 in 2004, the transition zone is highlighted in all directions.

#### 4. Conclusion

In this study, a wavelet-CNN was shown to be useful for classifying cross-sectional optical micrographs indexed by the year of the annual ring. This network may have a potential to extract structural information specific to a calendar year, which was previously thought to be impossible, even from visual scrutiny by experts. A comparison of wavelet-CNN and random forest methods suggests that wavelet-CNN may be used as dendroclimatology technique, because several tree ring studies using such tree growth parameters have reported interesting results regarding annual growth patterns and climate information. Although further studies using more samples from different individuals are required, the present study is the first successful deep learning approach to be applied to image data for tree ring analysis. Once a robust model has been established and correlated with climatic information, it may allow us to predict the record of sub-seasonal climatic information from the analysis of tree rings.

#### Acknowledgements

The authors thank Ashiu Experimental Forest, Field Research Center, Kyoto University, for providing the samples used in this study and Professor Hiroaki Kawashima, Graduate School of Informatics, Kyoto University, for his valuable discussion. We also thank Stuart Jenkinson, PhD, from Edanz Group ([www.edanzediting.com/ac](http://www.edanzediting.com/ac)) for editing a draft of this manuscript. This study was partly supported by a Grant-in-Aid for Scientific Research (Grant Numbers 25252033 and 18H05485) from the Japan Society for the Promotion of Science, RISH Cooperative Research (database) and RISH Mission Research V-IV.

#### References

- [1] Fritts H C 1976 *Tree Rings and Climate*. Academic Press, London
- [2] Fonti P and Garcia-Gonzalez I 2004 *Suitability of chestnut earlywood vessel chronologies for ecological studies*. *New Phytologist* **163** 77–86,

- [3] Wimmer R 2002 *Wood anatomical features in tree-rings as indicators of environmental change*. *Dendrochronologia* **20** 21–36
- [4] Corcuera L, Camarero J J and Gil-Pelegrin E 2004 *Effects of a severe drought on growth and wood anatomical properties of Quercus faginea*. *IAWA Journal* **25** 185–204
- [5] Fonti P, Heller O, Cherubini P, Rigling A and Arend M 2013 *Wood anatomical responses of oak saplings exposed to air warming and soil drought*. *Plant Biology* **15** (Suppl. 1): 210–219
- [6] Nabais C, Campelo F, Vieira J and Cherubini P 2014 *Climatic signals of tree-ring width and intra-annual density fluctuations in Pinus pinaster and Pinus pinea along a latitudinal gradient in Portugal*. *Forestry* **87** 598–605
- [7] Castagneri D, Fonti P, von Arx G and Carrer M 2017 *How does climate influence xylem morphogenesis over the growing season? Insights from long-term intra-ring anatomy in Picea abies*. *Ann. Bot.* **119** 1011–1020
- [8] Kobayashi K, Hwang S W, Lee W H and Sugiyama J 2017 *Texture analysis of stereograms of diffuse-porous hardwood: identification of wood species used in Tripitaka Koreana*. *J Wood Sci* **63**:322–330
- [9] Kobayashi K, Akada M, Torigoe T, Imazu S and Sugiyama J 2015 *Automated recognition of wood used in traditional Japanese sculptures by texture analysis of their low-resolution computed tomography data*. *J Wood Sci* **61**:630–640
- [10] Yadav A R, Anand R S, Dewal M L and Gupta S 2015 *Multiresolution local binary pattern variants based texture feature extraction techniques for efficient classification of microscopic images of hardwood species*. *Appl Soft Comput* **32**:101–112
- [11] Martins J, Oliveira L S, Nisgoski S and Sabourin R 2013 *A database for automatic classification of forest species*. *Mach Vis Appl* **24**(3):567–578
- [12] Wang H J, Zhang G Q and Qi H N 2013 *Wood recognition using image texture features*. *PLoS ONE* **8**(10): e76101
- [13] Lowe D G 1999 *Object recognition from local scale-invariant features*. In: *Proc. the Seventh IEEE International Conference on Computer Vision*. IEEE, Kerkyra, pp 1150–1157
- [14] Hwang S W, Kobayashi K, Zhai S and Sugiyama J 2018 *Automated identification of Lauraceae by scale-invariant feature transform*, *J Wood Sci* 64:69-77
- [15] Hwang S W, Kobayashi K and Sugiyama J Oct 26, 2018 *13th CKJ seminar*
- [16] Kobayashi K, Hwang S W and Sugiyama J Oct 26, 2018 *13th CKJ seminar*
- [17] Fujieda S, Takayama K and Hachisuka T 2018 *Wavelet Convolutional Neural Networks*, arXiv:1805.08620v1
- [18] Gärtner H., et al. 2015 *A Technical Perspective in Modern Tree-ring Research - How to Overcome Dendroecological and Wood Anatomical Challenges* e52337, doi:10.3791/52337
- [19] Otsu N 1975 *A threshold selection method from gray-level histograms*. *Automatica* **11**, 23-27
- [20] Sano Y in *Secondary Xylem Formation 2nd edition* (in Japanese ), Fukushima et al, Eds., 2003, pp53 (Kaiseisha, Shiga, Japan)
- [21] Jevšenak J, Džeroski S, Zavadlav S and LevaničA T 2018 *Machine Learning Approach to Analyzing the Relationship Between Temperatures and Multi-Proxy Tree-Ring Records Tree-Ring Research*, **74**(2):210-224.
- [22] Selvaraju R R, Das A, Vedantam R, Cogswell M, Parikh D and Batra D 2016 *Grad-CAM: Why did you say that? Visual Explanations from Deep Networks via Gradient-based Localization*. CoRR, abs/1610.02391